



Unexpected VLF Bursty-Patches Above 5 kHz: A Review of Long-Duration VLF Series Observed at Kannuslehto, Northern Finland

J. Manninen¹ · N. G. Kleimenova^{2,3} · C. Martinez-Calderon⁴ · L. I. Gromova⁵ · T. Turunen¹

Received: 13 April 2022 / Accepted: 14 September 2022 / Published online: 12 November 2022
© The Author(s) 2022

Abstract

Unexpected short patches of natural VLF emissions at $f > 5$ kHz have been observed at the ground station of Kannuslehto (KAN, $L \sim 5.5$) in Northern Finland. In contrast with usual VLF emissions (e.g., chorus, hiss, and quasiperiodic emissions) these high-frequency bursty-patches are observed at frequencies higher than half of the equatorial electron gyrofrequency of the L shell of KAN. Moreover, most of these waves reached frequencies above the local equatorial electron gyrofrequency at $L = 5.5$. Thus, they cannot be attributed to the classical theory of electron-cyclotron interaction. We present a review of VLF bursty-patches at KAN during winters 2011–2021. These emissions have rarely been observed as they are usually hidden by sferics originating from lightning discharges. Therefore, a special numeric filtering technique was used to reduce noise from sferics. VLF bursty-patches typically occur as sequences of short right-hand polarized bursts separated by a few minutes and lasting several hours. Here, we discuss the spectral structure of long-lasting bursty-patches (6+ hours) and the properties of individual patches. We established two categories: (1) “triggered-like” hiss-like bursts at $f \sim 4\text{--}7$ kHz with a very abrupt onset and detected under quiet geomagnetic conditions, and (2) “dash-like” emissions at $f > 6$ kHz that resemble narrowband hiss and observed under moderate activity. Even though VLF bursty-patches in winters 2011–2021 were observed under weak or slightly disturbed magnetic activity, their annual cyclical occurrence was similar to variations in solar activity. The nature of these VLF patches has not been established yet, but they appear to be generated at L shells lower than that of KAN. Their exact generation region and propagation behavior remain unknown, with further theoretical and experimental research being required.

✉ J. Manninen
jyrki.manninen@oulu.fi

¹ Sodankylä Geophysical Observatory, University of Oulu, 99600 Sodankylä, Finland

² Schmidt Institute of Physics of the Earth RAN, Moscow 123995, Russia

³ Space Research Institute RAN, Moscow, Russia

⁴ Institute for Space-Earth Environmental Research, Nagoya University, Nagoya 4648601, Japan

⁵ Pushkov Institute of Terrestrial Magnetism, Ionosphere and Radio Wave Propagation RAN, Moscow 142191, Russia

Keywords VLF waves · Electron cyclotron interaction · Geomagnetic disturbances

Article Highlights

- VLF bursty-patches are short bursts detected at frequencies higher than the local equatorial electron gyrofrequency (f_{ce}) at the L-shell of KAN ($f_{ce} \sim 5.4$ kHz)
- Triggered-like patches ($f \sim 4\text{--}7$ kHz) show an abrupt onset and are detected in quiet times. Dash-like patches present as narrow band emissions at $f > 7$ kHz during moderate geomagnetic activity
- Bursty-patches are generated in the magnetosphere via cyclotron instability in the equatorial plane at L shells much lower than KAN

1 Introduction

Natural whistler-mode electromagnetic waves in the very low frequency (VLF) range (3–30 kHz) are a typical phenomenon in the magnetosphere. Their generation is described by a whistler-mode electron cyclotron maser model as a generator or amplifier of waves along closed magnetic flux tubes filled with a dense cold plasma (Trakhtengerts and Rycroft 2008). These waves have been widely studied, in particular since the review by R. A. Helliwell (1965) featuring a rich collection of different spectral forms of VLF emissions observed mostly on the ground, but also within the magnetosphere and widely known as chorus, hiss, quasiperiodic (QP) and discrete emissions.

It is generally accepted that most VLF emissions are generated via electron cyclotron interaction of waves and energetic electrons of the radiation belts at the frequencies controlled by the electron gyrofrequency f_{ce} (Trakhtengerts 1963; Kennel and Petschek 1966; Rycroft 1972, 1991; Trakhtengerts and Rycroft 2008). From the wave generation source, located in the equatorial plane of the magnetosphere, the waves may propagate to the ionosphere in the waveguide regime described by Inan and Bell (1977) and Semenova and Trakhtengerts (1980), that is, guided by enhanced density gradients extended along the magnetic field lines. It was shown theoretically (Smith et al. 1960) and experimentally (Carpenter 1968) that ducted propagation of VLF waves is possible at frequencies lower than half of the equatorial electron gyrofrequency ($0.5 f_{ce}$) of any given L -shell. However, ducted propagation of VLF waves is also possible for whistler-mode waves with frequency $f > 0.5 f_{ce}$, but it requires rarefaction (depleted) ducts (e.g., Smith et al. 1960; Karpman and Kaufman 1982; Bespalov et al. 2022).

The waves with higher frequencies propagate non-ducted, meaning with oblique wave angles to the local magnetic field lines (e.g., Némec et al. 2013; Martinez-Calderon et al. 2016; Titova et al. 2017; Demekhov et al. 2020). Ducted VLF whistler waves which penetrate through the ionosphere with low wave normal angles with respect to the vertical, can be observed on the ground in the vicinity of the footprint of the ionospheric exit point of the wave (Helliwell 1965). Leaving the duct, right-handed elliptically polarized whistler waves penetrate into the Earth-ionosphere waveguide and can undergo many reflections from its anisotropic upper boundary. They can travel distances over ~ 800 km until they are detected by a ground-based receiver (e.g., Strangeways 1983). However, with increasing distance between the ionospheric exit point of the wave and its receiver, the right-handed polarization of the wave becomes left-handed (e.g., Yearby and Smith 1994). Thus, the right-handed polarization of the wave indicates that the receiver detecting the waves is

located in the vicinity of the ionospheric exit point, no further than 300–400 km. Despite the importance of direct VLF measurements in space with satellite instruments, continuous ground-based observations can provide a unique opportunity to study the temporal dynamics of the waves.

However, ground-based detection of high-frequency VLF emissions is difficult because, even at auroral latitudes, strong atmospherics (sferics) can completely mask natural emissions at frequencies above 4–5 kHz. Sferics are electromagnetic pulses originating from low latitude lightning discharges (e.g., Ohya et al. 2015) and propagating thousands of kilometers in the Earth-ionosphere waveguide. To remove this obstruction, a special digital program to filter out the strong impulsive sferics with a duration of less than 30 ms, has been applied to data from the ground-station of Kannuslehto (KAN) in Northern Finland. This method has been briefly described in Manninen et al. (2016). After filtering out the sferics, we surprisingly discovered completely new types of peculiar high-frequency (above 4–5 kHz) daytime VLF emissions with unusual spectral structures that have rarely been seen before (Manninen et al. 2016, 2017, 2021; Martinez-Calderon et al. 2021).

Figure 1 shows some examples of non-filtered (left) data and the same data after sferic filtering (right) as the 1-h total power spectrograms (frequency-time power spectra density distribution) on 3 different days. It is seen that the strong sferics hide all VLF signals at frequencies above ~5 kHz. After sferics filtering, the right panels clearly show multiple kinds of differently structured high-frequency VLF natural emissions. In these plots we also note a very intense low frequency band which corresponds to local power line harmonic radiation.

Previously, short bursts of high-frequency VLF emissions were detected by ground-based observations at $L \sim 4.3$ in Canada by Shiokawa et al. (2014) and called “bursty-patches.” These were believed to be related to upper band chorus emissions and were not studied in detail.

The first proper description of unusual high-frequency VLF bursts was published by Manninen et al. (2016, 2017) using data from KAN. A large quantity of these emissions was discovered after the application of a digital filter that filtering sferics out. At first, they were called “VLF birds” due to their sound resembling that of birds chirping and their dynamic spectra resembling flying birds. They were also referred to as “recently revealed emissions-RRE” (Manninen et al. 2016). Later on, following Shiokawa et al. (2014), the term “VLF bursty-patches” (Manninen et al. 2021; Martinez-Calderon et al. 2021) was established. Some spectral and morphological properties of these emissions, recorded at KAN in 2013–2021, have previously been discussed in (Manninen et al. 2016, 2017, 2021; Martinez-Calderon et al. 2021).

This review aims to summarize the general characteristics, spectral behavior, and geomagnetic situation during long-lasting series of unusual daytime “VLF bursty-patches” observed on the ground station KAN ($L \sim 5.5$) since 2006.

2 Instruments and Data Set

Our study was based on the VLF observations in Northern Finland at KAN, with the geographic coordinates 67.74° N, 26.27° E; which corresponds to the corrected geomagnetic latitude of 64.4°, i.e., $L = 5.46$ with a local equatorial electron gyrofrequency (f_{ce}) ~ 5.4 kHz.

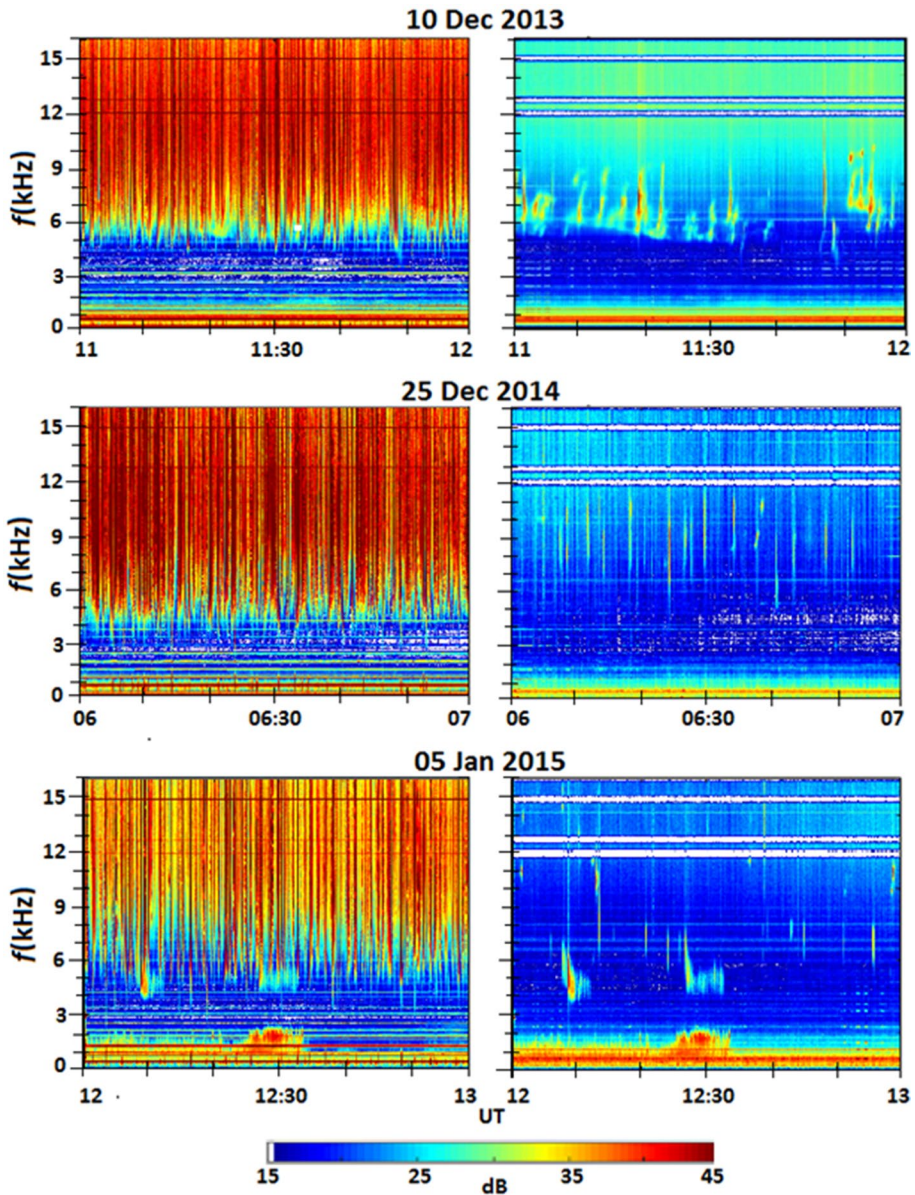


Fig. 1 Examples of 1-h dynamic spectrograms (0–16 kHz) of non-filtered (left panels) and filtered (right panels) VLF data at KAN during three different days. White horizontal lines above 11 kHz in the right panels are the removed radio navigation transmitter signals. Taken from Manninen et al (2016)

KAN station is located at a low-noise site approximately 40 km north of the Sodankylä Geophysical Observatory. The VLF receiver in the frequency band from 0.2 to 39 kHz is comprised of two orthogonal magnetic loop antennas oriented in the geographical north–south and east–west directions. The receiver sensitivity is about 10^{-14} nT² Hz⁻¹. The wide dynamic range of the receiver (up to 120 dB) allows detection of both very weak and

strong signals. Sampling frequency is 78.125 kHz. For more details on the equipment see Manninen 2005. The magnetic field intensities are calibrated using the method described by Fedorenko et al. (2014).

The VLF observation at KAN is run on a campaign basis, with several wintertime campaigns carried out between 2006 and 2021. The results of the primary VLF processing (Fast Fourier Transform) and filtered out sferics data can be found online in the form of minute, hour, and daily wave dynamic spectra (spectrograms at 0–16 kHz) at https://www.sgo.fi/pub_vlf/.

3 Observations

It has been established (Manninen et al. 2016) that VLF bursty-patches are right-hand polarized whistler mode short bursts (from a few tens of seconds to 1–2 min) at frequencies higher than 5–6 kHz, meaning at much higher frequencies than $0.5 f_{ce}$ and even above f_{ce} . They are observed predominantly during the daytime with an occurrence rate from 1–2 signals per hour to long-continued series of sequential bursts lasting several hours. This review focuses on the latter case.

Figure 2 shows two examples of the series of the sequences of VLF bursty-patches with a total duration of approximately 6 h each. Events of this long duration require the amplification of whistler mode waves in the magnetosphere to compensate for the losses due to nonideal ionospheric reflection and refractive spreading of the wave energy (Demekhov et al. 2021). The spectrograms in Fig. 2 demonstrate that majority of

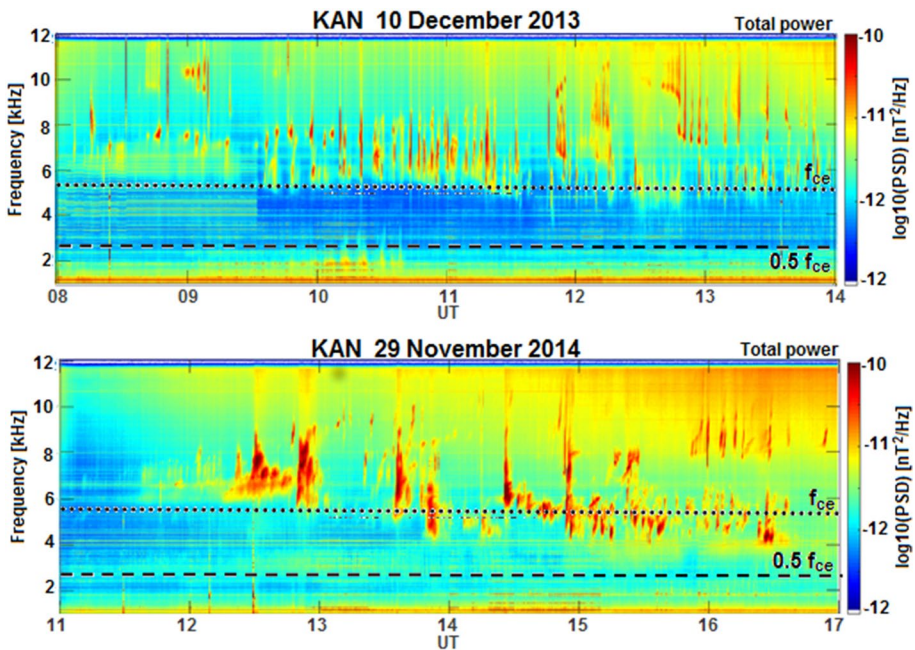


Fig. 2 Two examples of 6-h series of high-frequency VLF bursty-patches. The dotted and dashed horizontal white lines show the local equatorial electron gyrofrequency (f_{ce}) and $0.5 f_{ce}$ for the L -shells of KAN

these signals occur at frequencies higher than f_{ce} at the L shell of KAN (indicated by the horizontal dotted line). The spectrogram has a maximum frequency limited to 12 kHz to avoid the strong signals of radio navigation transmitters at higher frequencies, and a minimum frequency limited to 1 kHz to avoid electromagnetic noise.

We found that the long series of VLF bursty-patch sequences are typical for winter, i.e., for the dark season around the midwinter solstice of November to January (Manninen et al. 2016, 2017). This has been interpreted as the result of strongly asymmetric conditions in the magnetically conjugate ionosphere (Manninen et al. 2013). In the Northern (darker) ionosphere, the whistler mode wavelength appears to be comparable with the spatial scale of the plasma density gradient, whereas in the Southern (sunlit) ionosphere the wavelength is much smaller and accompanied by a stronger wave absorption in the D-region occurs.

3.1 Some Statistical Properties of High-Frequency VLF Bursty-Patches Observed at KAN

During the winter seasons 2011–2021 of VLF observations at KAN, we selected 52 events of long series of high-frequency bursty-patches lasting more than 1–2 h. We classified these emissions into two different spectral types: “*triggered-like*” emissions at frequencies below 7–8 kHz, and “*dash-like*” emissions at frequencies above 7–8 kHz. We use the term “*triggered-like*” VLF patches because the appearance of these waves simultaneously at all frequencies suggests the presence of some seed signal that triggers the generation of the observed burst, as in a classical trigger process.

We found 27 events of “*triggered*” and 17 events of “*dash-like*” VLF patches, with 8 complicated events when both types of VLF emissions were generated simultaneously or they cannot be attributed to “*triggered*” or “*dash-like*” cases.

All these VLF patches were recorded during the daytime under quiet or moderate geomagnetic activity. The global geomagnetic conditions during the considered VLF bursty-patches were estimated by the planetary Kp index. We found that during the “*triggered*” emissions, the value of the Kp index was mainly 1, sometimes reaching 2, and during the “*dash*” emissions it was mainly 2, sometimes reaching 3.

We also studied the ring current level as well as a substorm activity during the VLF patches, by following the SMR and SML indexes methods described by Bergin et al. (2020). These share the same methodology as $Dst/SymH$ and AL indexes (Gjerloev 2012; Bergin et al. 2020). This data is taken from the SuperMAG magnetometer system which includes more than 300 ground-based stations distributed around the Earth, i.e., the number of magnetometer stations is about 10 times larger than those used in the classical indices. We suggest that the level of substorm activity is very important for the generation of VLF emissions because the SML index enhancement indicates a new electron injection into the magnetosphere from the tail. This injection could increase the plausible resonant electron number, supporting electron cyclotron instability as the main source of VLF wave generation. In the following subsection, we will use the SML index for geomagnetic situation estimation.

The calculated average values of SML index during the “*triggered*” VLF bursty-patches was ~ 70 nT (exactly 68 ± 18 nT), and during the “*dash-like*” emissions it was ~ 200 nT (exactly 223 ± 88 nT).

Most of the VLF patches we studied showed that they were coming from just overhead the station. However, some of the events seemed to come from the East–West or

North–South directions. In these cases, we need a more detailed analysis that involves comparing with Lovozero station data located at a similar geomagnetic latitude about 400 km eastward. This will be the object of a future paper.

Below, we will discuss some of the most striking properties of VLF bursty-patches. At first (Sects. 3.2 and 3.3), we present the typical temporal dynamics showing examples of the two types: “*triggered*” and “*dash-like*” emissions. We show the existence of different temporal dynamics of individual “dash-like” bursts as signals with stable and increased frequency, and show the geomagnetic conditions during their occurrence. Sections 3.4–3.7 display some non-typical individual VLF bursty-patches with a different spectral-time structure to underline their diversity requiring further theoretical research. Section 3.8 indicates that the high-frequency VLF patches are generated not only isolated under non-disturbed geomagnetic conditions but sometimes also after the end of a strong burst of high-frequency hiss emissions as a continuation of VLF wave generation in the similar frequency band, probably, indicating their common generation location.

3.2 Event on December 31, 2018 (Fig. 3)

This event shown in Fig. 3, lasting about 6 h, is one of the most typically observed in terms of temporal dynamics of the signal frequency and its spectral structure. Figure 3a, b indicates that during the first hour (at 06–07 UT) the average frequency of the event gradually increased from $f > 0.5 f_{ce}$ to $f \sim f_{ce}$ and later on ($\sim 07:40$ – $08:30$ UT), the frequency even exceeded f_{ce} . After $\sim 09:50$ UT, a new set of VLF bursty-patches occurred with different spectral structures and at different frequencies.

By this time, not only the frequency has changed, but the signal arrival direction changed as well. As shown in Fig. 3b, before $\sim 06:30$ UT, the signals arrived mainly from the meridian direction (red). Later, up to $\sim 08:20$ UT, the arrival direction became more azimuthal (yellow-green), but after $\sim 09:30$ UT the direction of arrival changed back to the meridian direction (red). We suppose this could indicate different sources for the VLF bursty-patches observed at the beginning of this event and at the end. In the event beginning, the station could be located near the meridian of the ionospheric exit area of the waves. Then, due to the rotation of the Earth, the station gradually and azimuthally moves away from this area, and after about an hour KAN found itself near the meridian of a new ionosphere wave exit area. If the probable source of emissions is at low L where the cold plasma could corotate almost ideally, the observed change of the wave arrival direction confirms the existence of two separated wave sources at low L areas.

The typical spectral shape of the initial VLF bursty-patches ($\sim 06:30$ – $08:40$ UT) is shown in the left and middle panels of Fig. 3c in the time frame of a minute. They could be identified as “*triggered*” bursts with duration of about 20–30 s with a clear upper and lower frequency limit, and a sharp onset and ending. The triggered-like emissions look like a rising-tone chorus. A 10-s fine structure from the triggered-like VLF bursty-patches observed after $\sim 08:24:30$ UT (middle panels of Fig. 3c) is shown in Fig. 3d. Such rising structure is typical for triggered-like VLF bursts at any frequency band, but in different events, the frequency dispersion could be different.

On the other hand, the shape of the latter VLF bursty-patches ($\sim 09:40$ – $10:20$ UT) was completely different as shown in the right panel in Fig. 3c. Here, the signals looked like

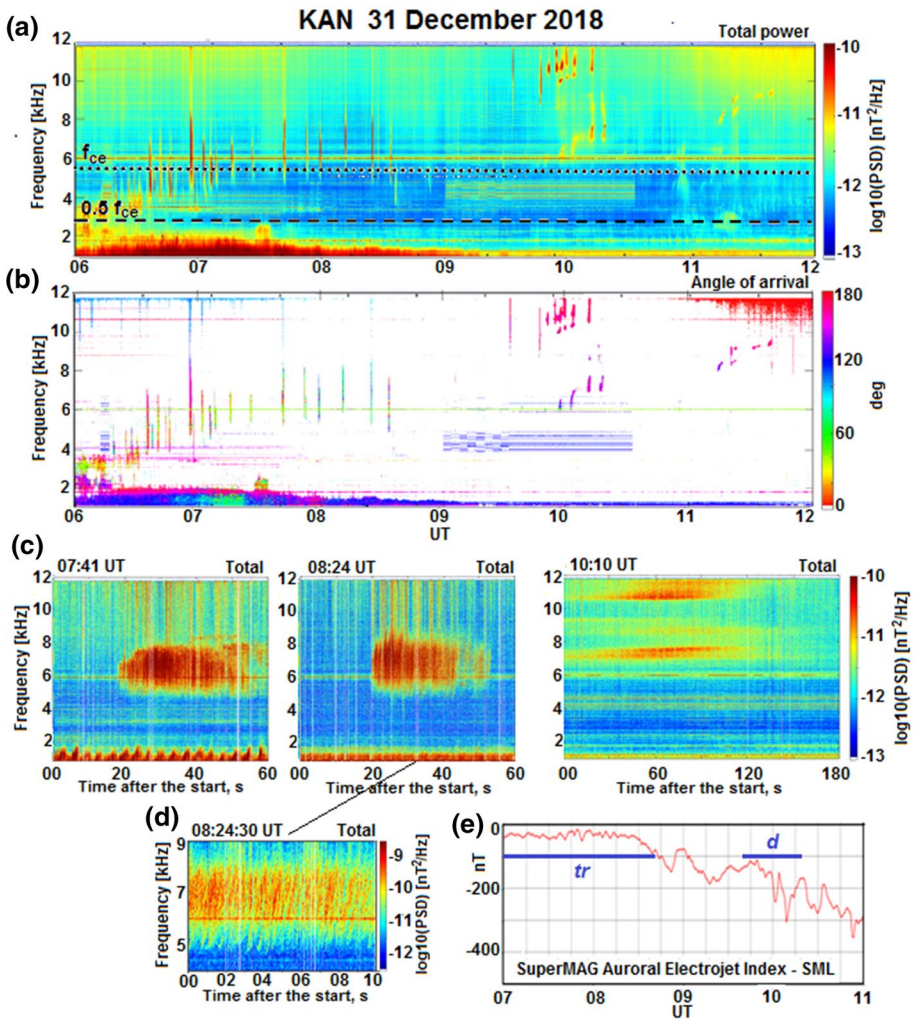


Fig. 3 The total power spectrogram (a) of the long-lasting event on December 31, 2018, showing the sequence of VLF bursty-patches. They are in the beginning of the event triggered hissy bursts at $\sim 5\text{--}7$ kHz (until $\sim 08:40$ UT) and changed to dash-like narrow band emissions higher than 6 kHz after $\sim 09:30$ UT; (b) The angle of arrival direction spectrogram, (c) examples of VLF bursts during the first (“triggered”) bursts and second (“dash-like”) emissions parts of the event; (d) 10-s spectrogram of the fine structure of the “triggered” VLF bursty-patch resembling the rising structure of chorus; (e) The geomagnetic activity, represented by the SuperMAG auroral electrojet SML-index

short (a few tens of seconds) “dash” lines with a rather narrow frequency range. In Martínez-Calderon et al. (2021), VLF emissions with such spectral shape were called “rounded VLF bursty-patches,” as they appear as round shapes in the 1-h spectrograms. In the right panel of Fig. 3c there are two “dash” patches with central frequencies of ~ 7 kHz and at ~ 11 kHz generated simultaneously, suggesting they have the same origin.

Figure 3e demonstrates that during the first part of the event under consideration, when the “triggered” bursts of the VLF bursty-patches have been observed, the

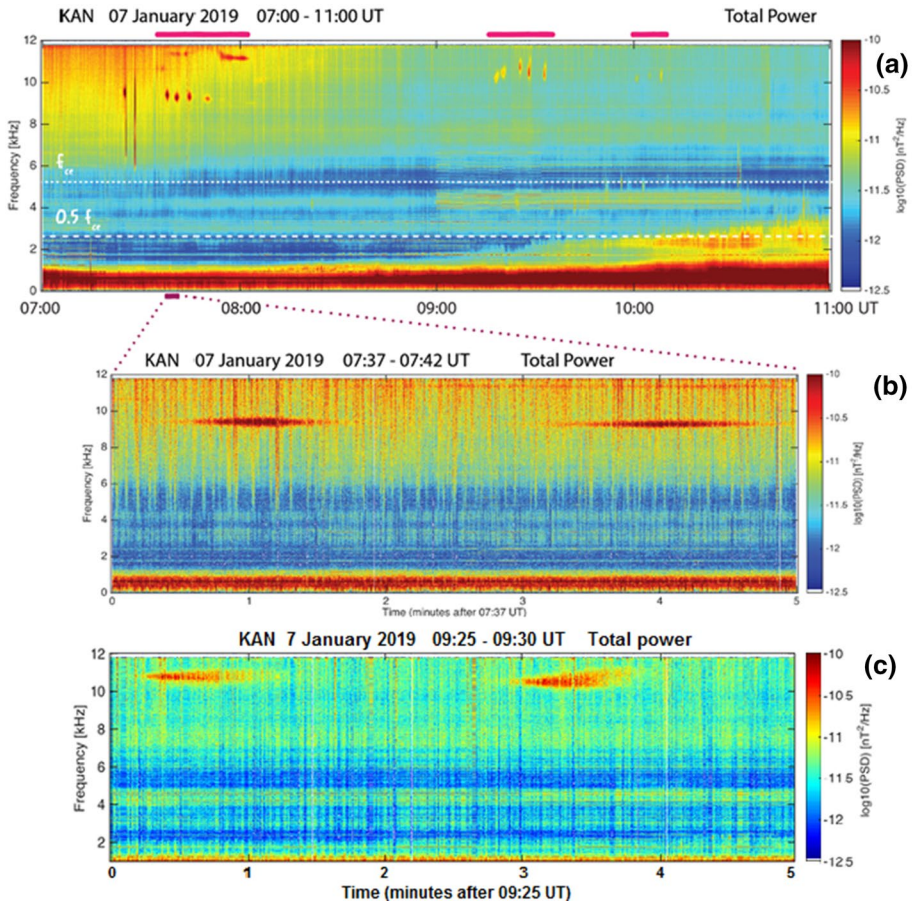


Fig. 4 An example of the power spectrograms of the series of “dash-like” VLF bursts observed at KAN on January 7, 2019: (a) between 07:00 and 11:00 UT and (b) between 07:37 and 07:42 UT (in the beginning of the event). (c) The VLF emission from 09:25 to 09:29 UT (in the end of the event). Figure is adapted from Martinez-Calderon et al. (2021) adding the bottom panel showing an additional time frame for the same event

geomagnetic activity was very low (*SML*-index \sim -100 nT). However, during the final part of the event (\sim 10 UT), the values of the *SML*-index changed to $-(250\text{--}300)$ nT. So, the “dash-like” VLF patches are generated under enhanced geomagnetic activity.

3.3 Events on January 7, 2019, and January 19, 2021 (Figs. 4 and 5)

The two long-lasting VLF bursty-patches events shown in Fig. 4 and Fig. 5 represent a series of the “dash-like” emission generation. Both events have been discussed in detail by Martinez-Calderon et al. (2021). We note that the “dash” VLF bursts look like thin sticks or spots in a time scale of several hours (Figs. 4a and 5a) but look like horizontal dashes in a time scale of minutes (Figs. 4b-c and 5b-c).

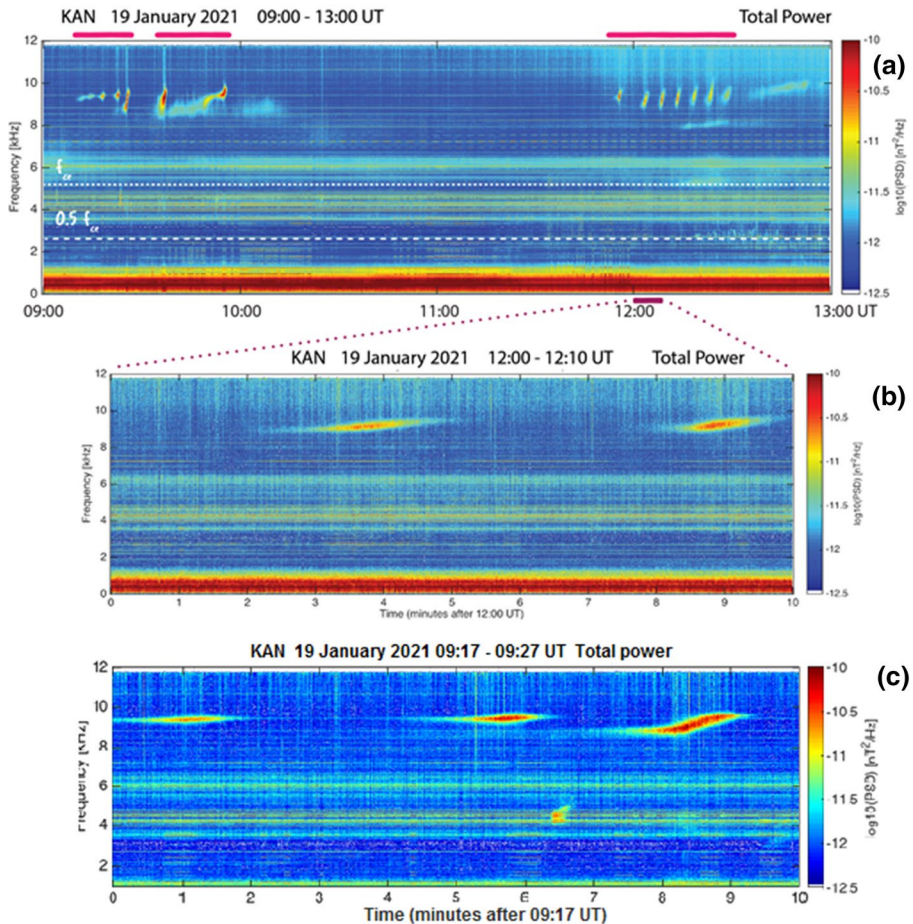


Fig. 5 Another example of the series of dash-like VLF bursts observed at KAN on January 19, 2021: (a) between 09:00 and 13:00 UT and (b) between 12:00 and 12:10 UT (in the end of the event). (c) VLF emission from 09:17 to 09:27 UT (in the beginning of the event) showing “S-shape” “dash-like” emissions. Figure is also reproduced from Martinez-Calderon et al. (2021) with the addition of panel (c) showing another time frame of the event

The first event (January 7, 2019) shows the “dash-like” emissions with a stable frequency throughout each signal burst, while the second event (January 19, 2021) shows “dashes” with increasing frequency with each burst. The two upper plots in Fig. 4 and Fig. 5 present spectrograms adopted from Martinez-Calderon et al. (2021), while the bottom plots show the spectrograms of the VLF bursty-patches observed near the end of the first event (09:25–09:30 UT) and in the beginning of the second event (09:17–09:27 UT). Both patches were observed near local magnetic noon.

Comparing the 5-min spectrograms on January 7, 2019, shown in Fig. 4b and 4c, one can see that the average frequency of the “dash” signals changed from ~9 kHz (07:37–07:42 UT) to ~11 kHz (09:25–09:30 UT). That is also clearly seen in Fig. 4a showing the 4-h spectrogram. In all figures we can see the enhancement of the frequency band. The frequencies of this emission were much higher than the equatorial f_{ce} of KAN. During

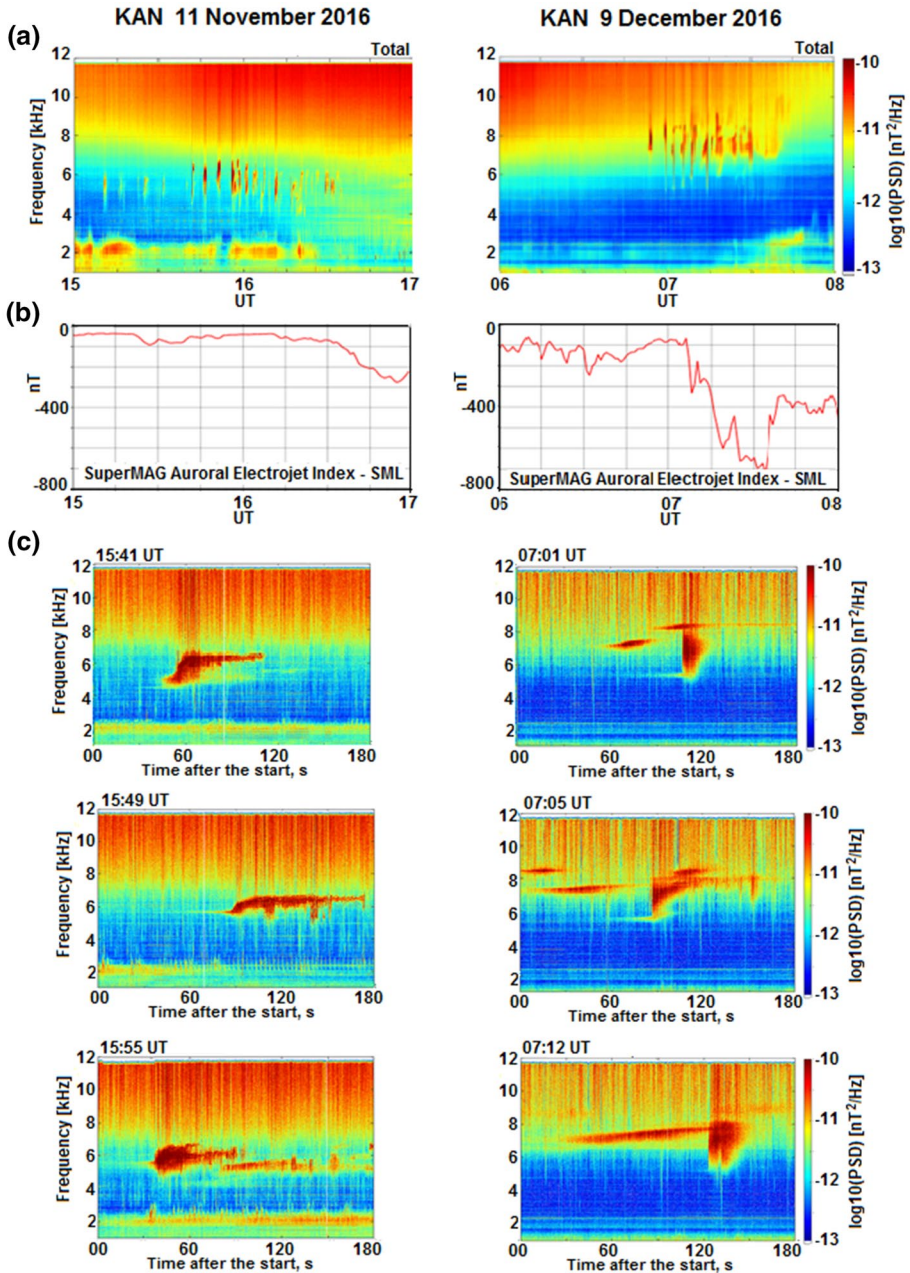


Fig. 6 The comparison of two VLF bursty-patch events (November 11, 2016, and December 9, 2016) showing the evening (15–17 UT, i.e., 16:30–18:30 MLT) emissions at frequencies below ~7 kHz and the morning (06–08 UT, i.e., 07:30–09:30 MLT) ones at frequencies above ~7 kHz: (a) 2-h total power spectrograms, (b) 2-h geomagnetic activity representing the SuperMAG auroral electrojet *SML*-index; (c) 3-min total power spectrograms selected of both events discussed above

the second event (Fig. 5), the frequency of the “dash-like” VLF bursts tended to increase with time with each additional signal. As seen in Fig. 5c, the shape of the individual bursts is smeared out to resemble that of an elongated letter “S” (Martinez-Calderon et al. 2021). It is interesting to mention that the first event with the stable frequency was observed under quiet geomagnetic conditions (*SML* index ~ -100 nT) but the second one with increased frequency was observed under enhanced geomagnetic activity (*SML* index ~ -450 nT).

3.4 Events on November 11, 2016, and December 9, 2016 (Fig. 6)

Figure 6a shows 2-h spectrograms of two events that are rather similar. The first one was observed in the late evening as a series of stick-like bursts at frequencies lower than ~ 7 kHz. The second event was observed in the late morning (before noon) at frequencies higher than ~ 7 kHz. Several individual signals of these events are shown in Fig. 6c. Some new spectral shapes are seen in both cases, but the “dash-like” VLF bursts were observed only in the second event at frequencies above ~ 7 kHz.

In the first event (left panels in Fig. 6c), the individual burst had a relatively clear flat top frequency just below 7 kHz. We attributed these signals to the “triggered-like” VLF emissions although they did not have a sharp onset. Moreover, some of these bursts had a narrow short “nose” at the front of it at a frequency of about 6 kHz. In the second event (right panels in Fig. 6c), a superposition of “dash-like” signals and short “triggered-like” bursts with a very abrupt onset was observed, the lower frequency of which decreased rapidly over time.

The comparison of the geomagnetic conditions during both events (Fig. 6b) shows that the “dash-like” VLF bursty-patches were observed under much higher geomagnetic activity than those below ~ 7 kHz. A similar tendency is also shown in Fig. 3, where the “trigger-like” emissions appeared under rather quiet geomagnetic conditions, while the “dash-like” emissions developed under moderate geomagnetic disturbances.

3.5 Event on January 5, 2017 (Fig. 7)

A series of VLF bursty-patches were observed near local noon at frequencies above ~ 7 kHz as presented in Fig. 7. This event is similar to the previous one on December 9, 2016; however, in this case the VLF signals showed a broader frequency band that may indicate a rapid frequency increase with the time of each burst. This is shown in detail in Fig. 7b, namely, in the time interval of 09:02–09:12 UT.

At this time, the signals show unusual ending features that are more clearly displayed in Fig. 7c. The signal ends look more like an overlay of “triggered” and “dash” VLF bursty-patches. Moreover, as shown in Fig. 7c at 09:14–09:17 UT, we detected the simultaneous occurrence of the “dash-like” and the strong “triggered-like” VLF bursts with a very sharp onset and quasiperiodic spectral structure. However, it is not clear if this is a random signal overlapping or if the “triggered” burst generation is caused by the “dash-like” signals.

Figure 7d demonstrates that the occurrence of the frequency enlarged VLF bursty-patches at about 09:00–09:15 UT coincided with a small increase in the magnetic activity. This confirms once again that “dash-like” VLF bursty-patches are excited under a higher level of the magnetic activity compared to “triggered-like” VLF patches.

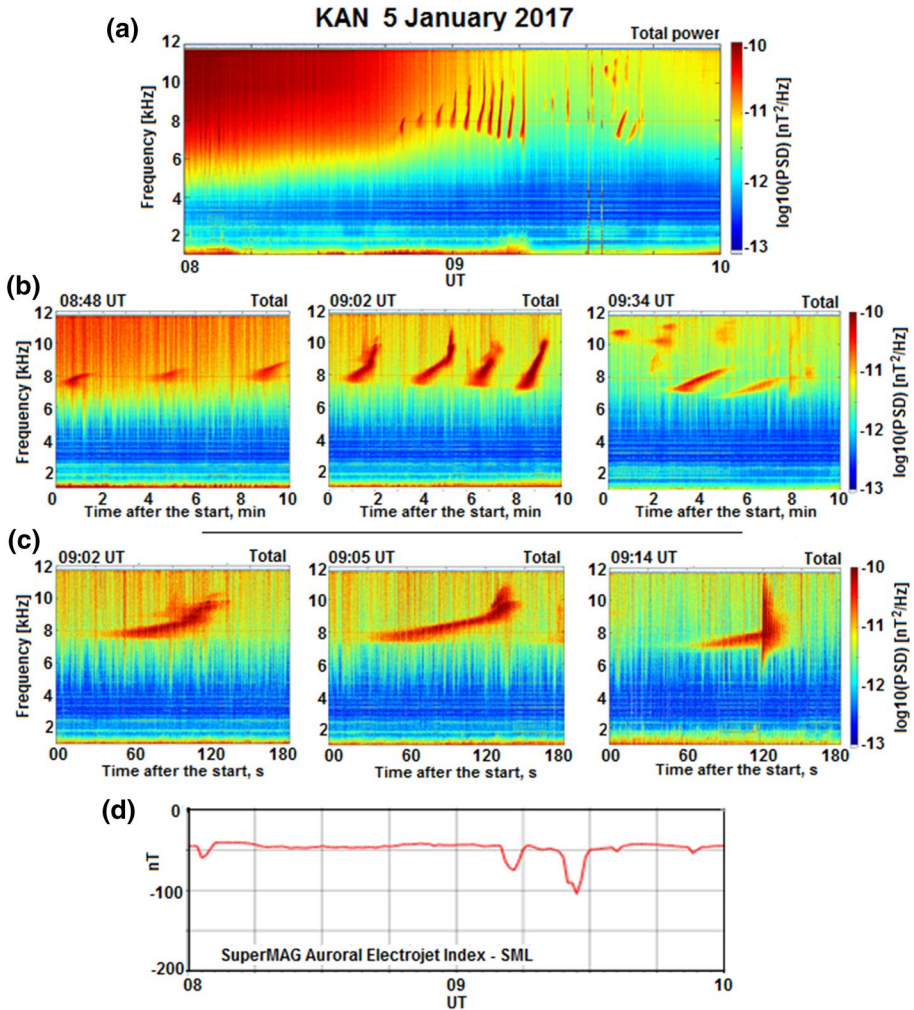


Fig. 7 An example of spectral evolution of the dash-like VLF bursts from ~08:40 to ~09:50 UT at KAN on January 5, 2017, between 08 and 10 UT: (a) 2-h total power at 08–10 UT; (b) and (c) 10-min and 3-min spectrograms selected during the studied event (description in the text); (d) 2-h geomagnetic activity representing the SuperMAG auroral electrojet SML-index

3.6 Event on January 28, 2017 (Fig. 8)

This event displayed in Fig. 8 was similar to the event on December 31, 2018 (Fig. 3). Both of them demonstrate the typical occurrence of the main types of the VLF bursty-patches: “triggered-like” emissions at frequencies below 7–8 kHz, and “dash-like” emissions above 7–8 kHz. The frequency range of spectrograms shown in Fig. 8 is 0–16 kHz because some VLF bursty-patches were observed at ~10–13 kHz at 08:46 – 08:49 UT (right upper panel in Fig. 8b). In this case, each burst lasted about 2 min and showed a hiss-like spectral structure. In this short time scale, they resemble the “wand” type emissions described by Fig. 4b

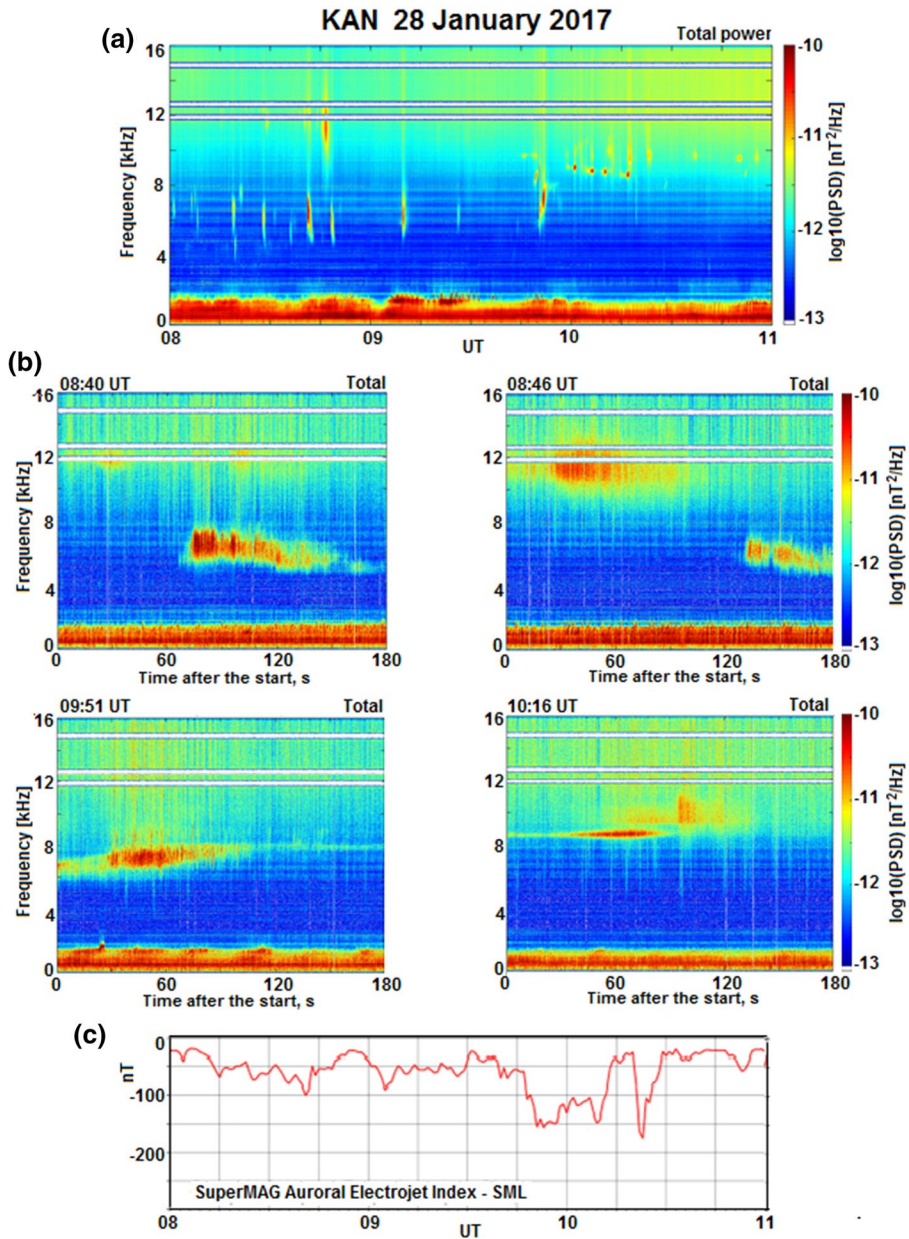


Fig. 8 (a) A 3-h total power spectrogram on January 28, 2017. Triggered bursty-patches below 8 kHz were observed mainly before local noon (~10 UT) and “dash-like” emissions above 8 kHz were observed mostly after noon; (b) 3-min spectrograms before and after the local noon; (c) The geomagnetic activity representing the SuperMAG auroral electrojet *SML*-index

of Martinez-Calderon et al. (2021) but at a lower frequency range (5–9 kHz). We note that on the 1-h spectrograms, these VLF bursts appear as vertical “wands” or sticks.

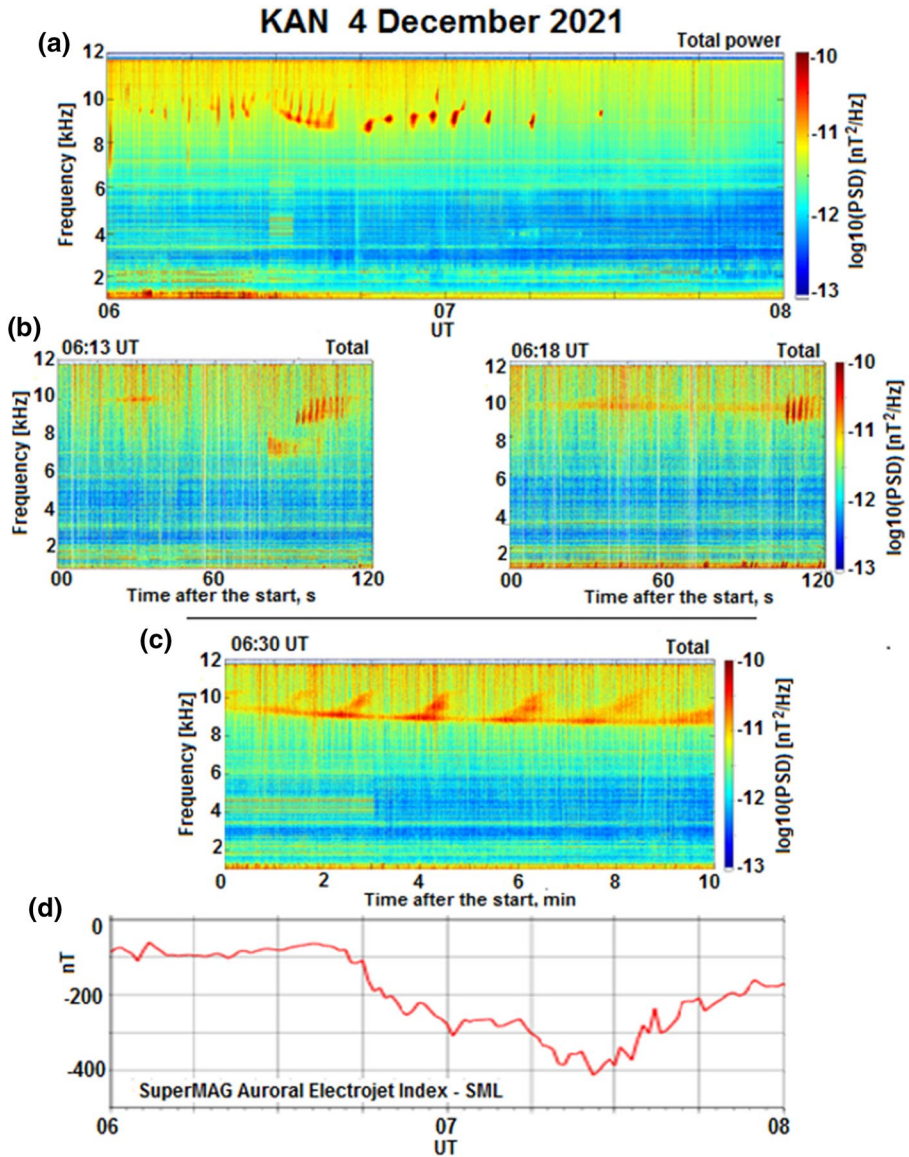


Fig. 9 (a) 2-h total power spectrogram at 06–08 UT on December 4, 2021; (b) 2-min spectrograms in the beginning of the event; (c) a 10-min spectrogram in the middle of the event; (d) the substorm activity according to the SuperMAG auroral electrojet *SML*-index

At the beginning of this event, up to ~ 10 UT, the short VLF bursty-patches have been observed at frequencies below ~ 7–8 kHz with a duration of about 1-min. Three examples of the spectrograms of these VLF patches are displayed in Fig. 8b. These emissions had a hiss-like structure with rising tones. After ~ 10 UT, a series of multiple “dash-like” VLF bursty-patches appeared at frequencies above 8 kHz (one example is shown in last panel

of Fig. 8b). As in the previous events, the “dash-like” emissions appeared with a moderate increase in the magnetic activity (Fig. 8c).

3.7 Event on December 4, 2021 (Fig. 9)

Figure 9a shows one of the most recent cases with a total duration of fewer than 2 h. Two unexpected and unusual VLF bursty-patches have been recorded during this event.

The event started as a series of short VLF patches in the frequency band of ~7–10 kHz. The 2-min spectrograms from 06:14 to 06:20 UT shown in Fig. 9b indicate the appearance of two short (~10–20 s) periodic VLF patches with a periodicity of ~2 s. These look like typical periodic emissions (*PEs*) described by Engebretson et al. (2004) based on observations at five Antarctic stations covering a range of magnetic latitudes from ~62° MLAT (Halley) to ~74° MLAT (South Pole Station). The Antarctic *PEs* have been observed at frequencies below ~3–4 kHz and were restricted to the dayside. They occurred more frequently at subauroral latitudes with a periodicity of a few seconds, similar to the two-hop travel time of echoing whistlers at the same frequency. Later on, similar emissions were observed by the DEMETER satellite (Bespalov et al. 2010) at frequencies below 2.5 kHz and they were interpreted as periodic auto-oscillations of the magnetosphere maser.

Here, we show for the first time, periodic VLF emissions (*PEs*) detected at such high frequencies as 9–10 kHz. Such phenomena have not been studied in detail enough, yet, but we have to keep in mind that Bespalov’s (2010) mechanism of passive mode locking is not restricted to any particular frequency range and can work in any frequency range where the emissions are generated. We hope that future theoretical works could shed light on this observed fact.

VLF bursty-patches were also observed during this event at ~06:30–06:40 UT (Fig. 9a). The series of signals were recorded at KAN at frequencies above 9 kHz, the outlines of which resemble an inverted hair comb. This can be seen in more detail in Fig. 9c depicting 10-min spectrograms of these emissions. The figures show simultaneous generation of the “dash-like” VLF patches with a very narrow frequency band (~9.0–9.5 kHz), and the overlapping short bursts of hiss-like emissions with quickly increasing frequency and bandwidth (~9–11 kHz). The hissy bursts were exited above each “dash” signal, which could suggest a causal relationship between them. Currently, there is no reasonable explanation for the generation of such complicated emissions.

In Fig. 9d, we display the correspondent variation of substorm activity according to the *SML* index. It is seen that *PEs* recorded during 06:14–06:20 UT were observed under very quiet geomagnetic conditions before substorm onset. On the other hand, the second comb-like quasiperiodic VLF bursty-patches appeared at 06:30–06:40 UT with a repetition period of about 1.5 min during the substorm growth phase just before the substorm onset which “switched off” the wave generation. Several short hissy VLF patches looking like the sequences of dots were generated during this substorm, but we did not observe a similar situation on other days. Therefore, we cannot say if this is a typical situation or not. As this is the first time such results are published, there is still no logical theoretical interpretation of this observational fact.

The *PEs* emissions at 8–9 kHz were typically observed at KAN during daytime under quiet geomagnetic conditions. However, the QP2 VLF patches at such high frequency with repetitions of a few minutes can be observed during disturbed times as well. For example, on December 5, 2014, at 05–06 UT during a substorm with an *SML* index of about -400

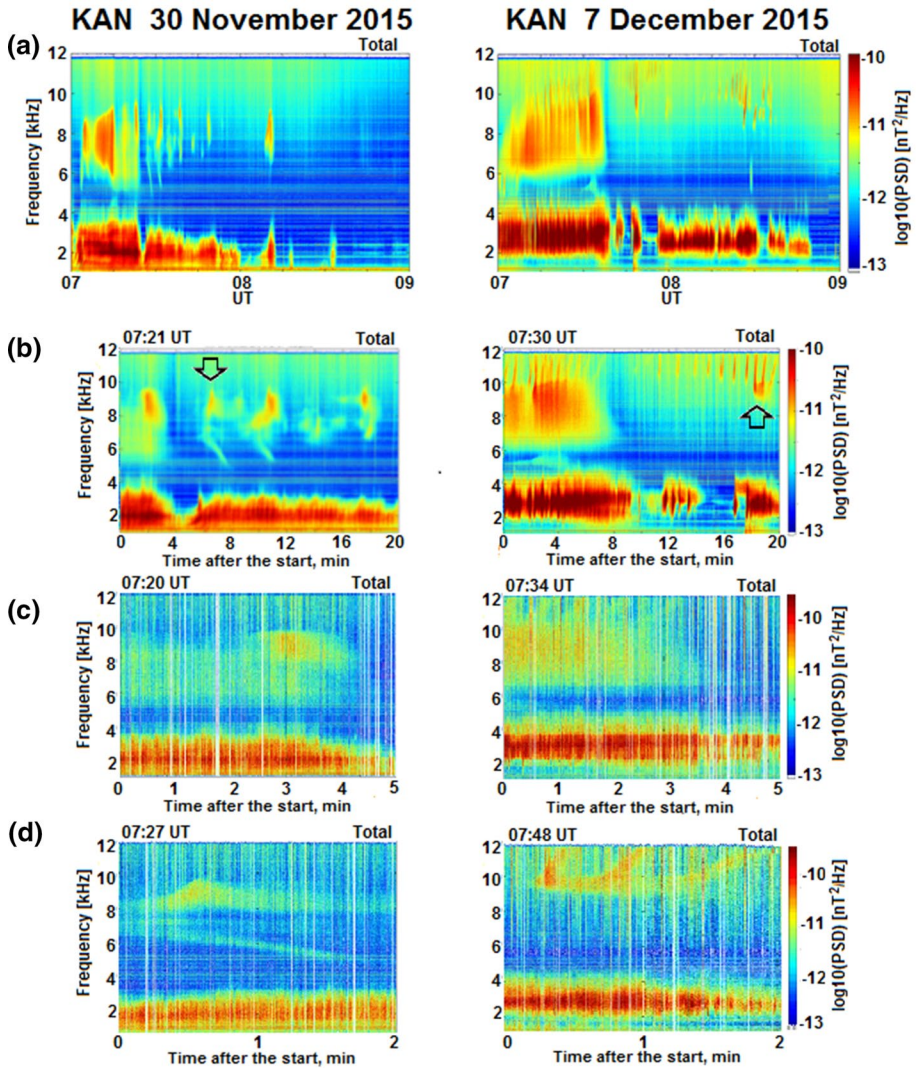


Fig. 10 Two relatively similar VLF events during which the high-frequency bursty-patches occurred after strong ~6–10 kHz bursts of hiss emissions on November 30, 2015, and on December 7, 2015: (a) 2-h total power spectrograms of both events at 07–09 UT, (b) 20-min spectra of selected VLF patches during both events; (c) The as b in a 5-min scale; (d) 2-min spectra of strange VLF-patches occurring after the end of the hiss burst

nT. Thus, a quasiperiodic structure of high-frequency VLF bursty-patches with different time-scale of the signal repetition (from a few seconds to a few minutes) requires a more detailed analysis.

3.8 Events on November 30, 2015, and December 7, 2015 (Fig. 10)

Figure 10 shows two events with similar features observed before local magnetic noon. The series of high-frequency (above ~ 7 kHz) VLF bursty-patches were recorded after a solid 6–9 kHz hiss was suddenly suppressed how it looks in the 2-h spectrogram in Fig. 10a. However, the 20-min spectrograms (Fig. 10b), as well as the 5-min ones (Fig. 10c), show that the suppression was not instantaneous. It can be seen in Fig. 10c that the hiss intensity decreased gradually between 07:23 and 07:25 UT in the first event, and between 07:37 and 07:38 UT in the second event.

In the first event (November 30, 2015), just before the hiss ends, there was a short “dash-like” VLF bursty-patch at the frequency band of ~ 7.5 –9.0 kHz, i.e., near the top of the “dense cloud” hiss (Fig. 10c). The dash-like VLF bursty-patches continued after the end of the hiss for at least 20 min in the same frequency range as the previous hiss, supporting the same location of generation of both the “dense cloud” hiss and “dash-like” VLF bursty-patches.

The 20-min spectrograms of the VLF bursty-patches are displayed in Fig. 10b and show some sequence of hiss spots with the maximum intensity at ~ 8 –9 kHz. They seem to occur simultaneously with the intensity maxima of lower frequency (1–4 kHz) hiss. The very complicated spectral shape of the two first VLF bursts (at 07:27–07:32 UT) is also seen as well in Fig. 10b. They were not previously seen and could not be attributed to typical VLF bursty-patches. The fine structure of these VLF bursty-patches, shown in Fig. 10c by arrow, is displayed as a 2-min spectrogram in Fig. 10d.

During the second event (December 7, 2015), the VLF bursty-patches following the solid hiss burst were recorded at much higher frequencies (~ 9 –12 kHz) and resembled quasi-periodic occurrence of “dash-like” bursts with a quick increase in frequency from ~ 9 kHz to ~ 12 kHz. Even at the beginning of the event ($\sim 07:15$ –07:35 UT), these VLF emissions overlapped the body of the solid hiss burst. However, the visible correlation of the periodicity in the appearance of the VLF bursty-patches with quasi-periodic emissions observed simultaneously at frequencies below 4 kHz is not detected. The fine structure of these VLF bursty-patches observed at 07:48–07:51 UT, is shown in Fig. 10b demonstrating the quick increase in frequency from ~ 10 kHz to ~ 12 kHz.

The geomagnetic conditions during both events were moderately disturbed with *SML* index \sim –(150–180) nT during the first event, and \sim –(200–250) nT (not shown here).

4 Discussion

We have identified two major categories of spectral structures of high-frequency short VLF bursty-patches represented by long series of VLF emissions with a total duration of several hours. They are the “triggered-like” emissions at frequencies below 7–8 kHz and the “dash-like” emissions at frequencies above 7–8 kHz.

The first type is the short isolated “triggered-like” bursts, each lasting from tens of seconds up to a few minutes and consisting of closely spaced rising elements (Manninen et al. 2021). These emissions are characterized by a very sharp onset and clear boundaries of the frequency band. Most often these VLF bursts are observed in the frequency range of about 4–6 kHz, and sometimes they can be detected in the frequency band of ~ 5 –7 kHz. The main bodies of the bursts usually developed very rapidly and then gradually weakened with time. Some examples of the typical dynamic spectra of the “triggered”-like patches are

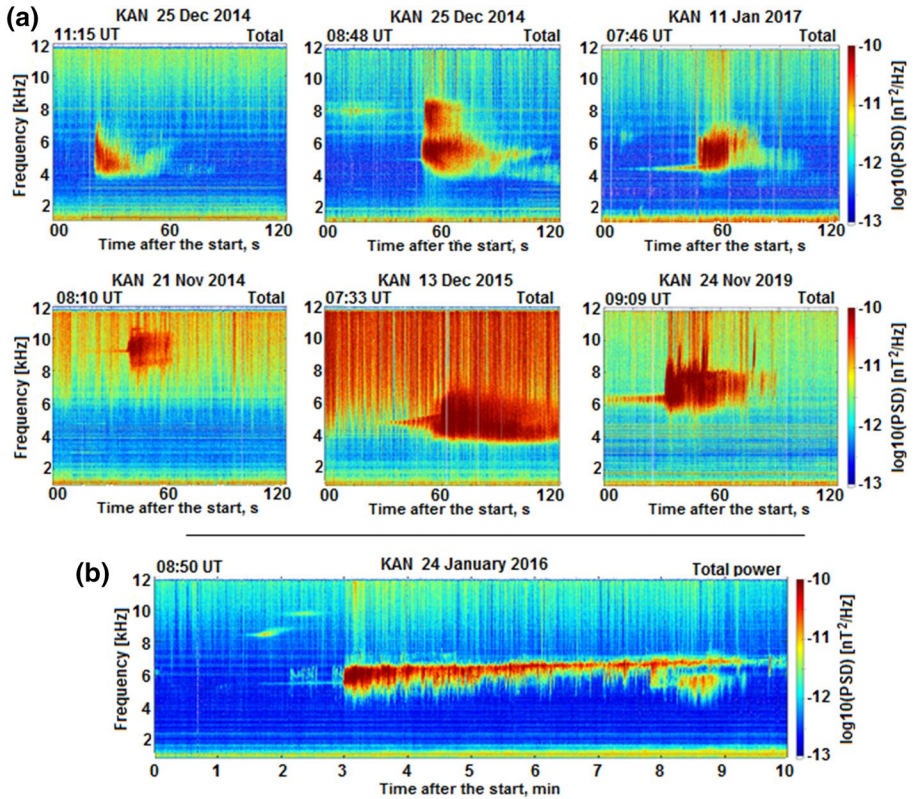


Fig. 11 (a) Six examples of 2-min spectrograms of different VLF triggered-like patches observed at KAN; (b) a 10-min spectrogram shows quite sharp upper cutoff of the event near 7 kHz

shown in Fig. 11 as 2-min VLF spectrograms. All these events have been observed under quiet geomagnetic conditions with an approximate *SML*-index of -100 nT. The VLF patch in Fig. 11, top middle, is shaped like a triangle showing a very quick frequency decrease. The VLF patch, top left, demonstrates the simultaneous occurrence of two separated frequency bands at ~4–6 kHz and ~6.5–8.5 kHz.

The next four spectrograms (top right and middle row) show an interesting feature of the “triggered-like” VLF bursty-patches: a long “nose” of a very narrow-band hiss preceding each patch by a few minutes and becoming progressively stronger with time. This “woodpecker nose” is a very common spectral structure indicating that this narrow-band frequency precursor is a necessary condition for the further development of the triggering mechanism of these VLF patches. The frequency of the “nose” precursor corresponded to the central frequency of the subsequent burst, or in some cases, to the lower frequency cutoff (last panel of the top row). In the middle row of Fig. 11, the spectrograms show very short period modulations of the narrow-band “nose,” especially in its beginning edge. We note, that a similar very narrow long “woodpecker nose” has been previously observed near the plasmapause about 49 years ago (in Sep 1973) by Dingle and Carpenter 1981. Their Fig. 3 shows (not shown here) the short noise burst directly triggered by whistlers propagating inside the plasmasphere in the top spectrogram.

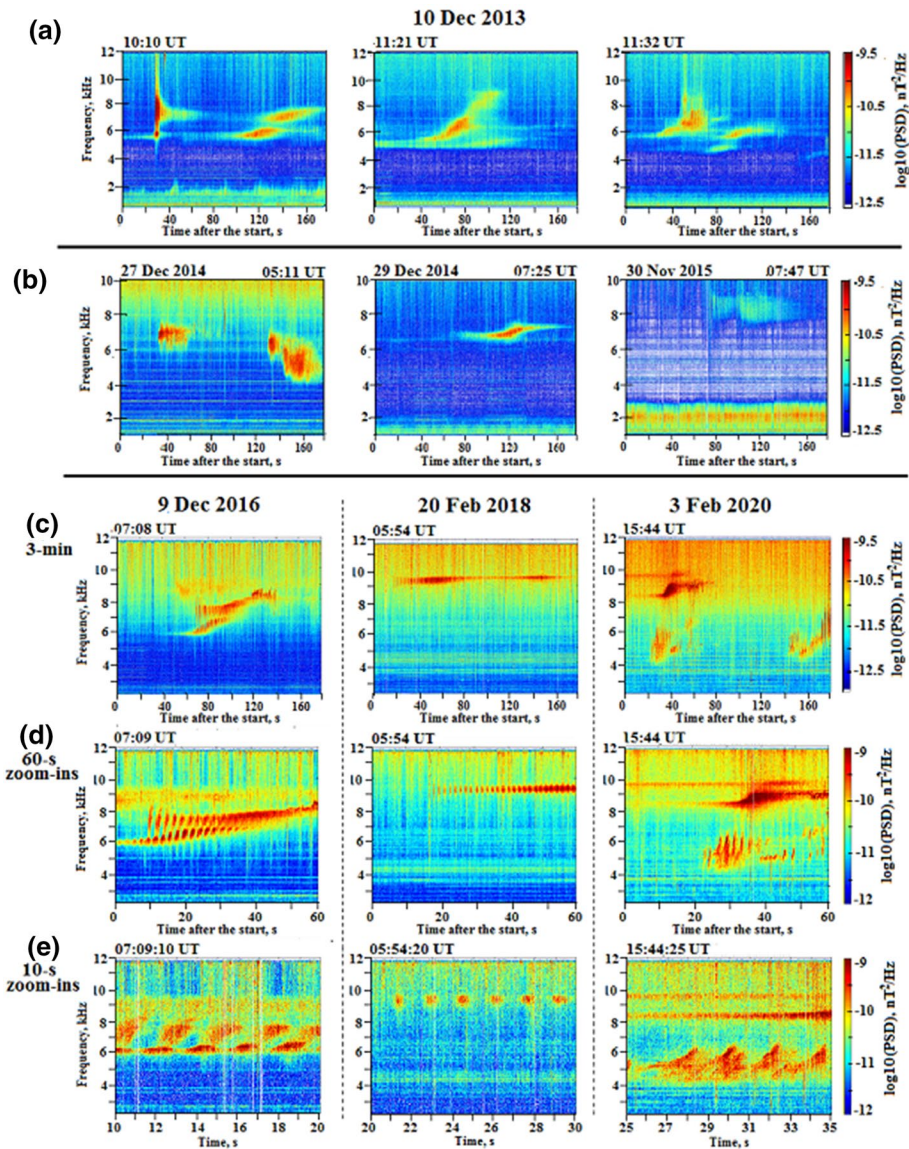


Fig. 12 Examples of different spectral structures of VLF patches observed at KAN. **(a)** 3-min spectrograms of the VLF patches with a sharp low frequency cutoff on December 10, 2013. **(b)** Typical spectral shapes of the VLF patches. **(c)–(e)**. Very complicated spectra of the VLF patches on three different days; **(c)** 3-min spectra **(d)** 1-min spectra detailing 3-min events; **(e)** Same in 10-s scales. Adopted from Manninen et al. (2021)

The bottom row of Fig. 11 shows a 10-min spectrogram with an example of a non-typical “triggered-type” VLF patch. It lasted about 6 min with an “inverted” spectral shape, meaning a clear upper-frequency cutoff at ~ 7 kHz rather than a lower cutoff, as is the case

in typical events. There was no significant difference in the geomagnetic conditions during this event and previously mentioned events.

The short VLF bursty-patches at the frequencies below 7–8 kHz often have curious spectral shapes as it was discussed by Manninen et al. (2016, 2021). Some of these spectrograms are presented in Fig. 12, adopted from Manninen et al. (2021). Figure 12a–c shows 3-min spectrograms of different VLF bursty-patch shapes. The dynamic spectra shown in Fig. 12a, with some imagination, may resemble flying birds and their sound resembles that of birds chirping; therefore these VLF patches were originally called “VLF birds.” Figure 12c shows examples of three different shapes of the 3-min spectrograms on different days. Figure 12d and e illustrates the fine spectral structure of these events by scaling to 60 s and 10 s, respectively. In the left panels of Fig. 12c–e (December 9, 2016), the very complicated dynamic spectra of the VLF patches demonstrate the short-period quasi-periodic modulation of the signal intensity at different frequencies simultaneously known as periodic emissions (PE). The spectrograms in the right panels in Fig. 12c–e (February 3, 2020) present the simultaneous generation of very complicated VLF bursty-patches with different durations and frequency bands (from ~4 kHz to ~10 kHz). Narrow-band “dash-like” VLF patches are at the top and the QP emissions are in the frequency

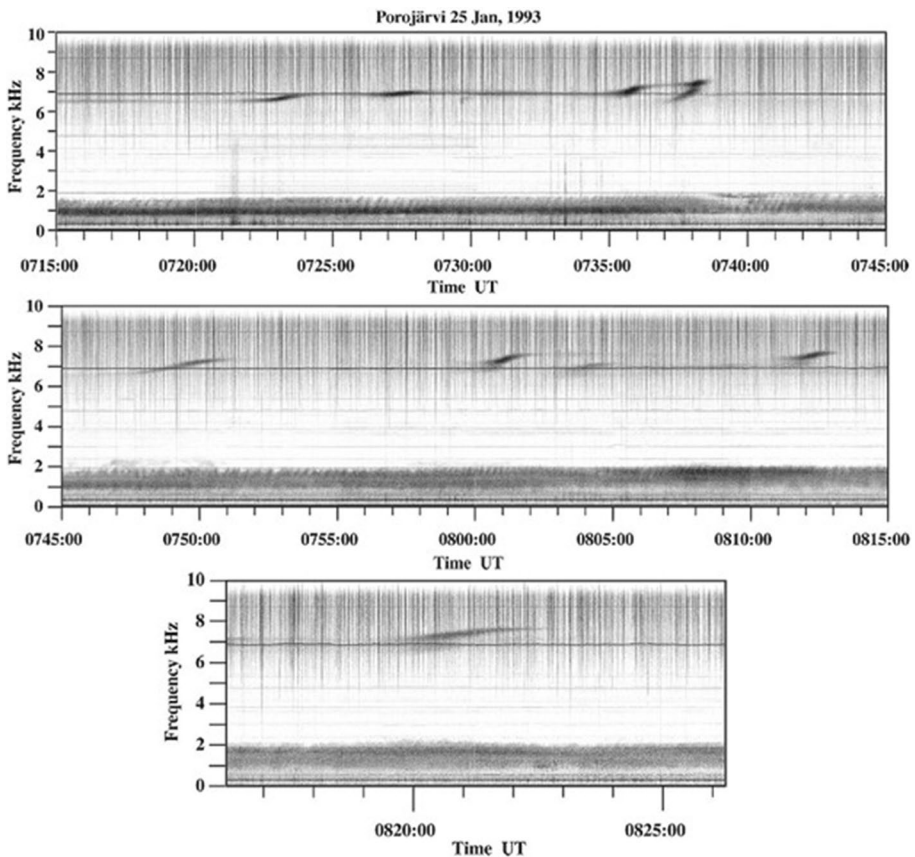


Fig. 13 High-frequency narrow band hiss events above 6 kHz observed in northernmost Finland on January 25, 1993. Taken from Manninen (2005)

band of ~4–6 kHz. Such complicated frequency-time evolution suggests that in different domains of the magnetosphere, different regimes of plasma instabilities can develop simultaneously.

The analysis of the variability of dynamic wave spectra is an important tool for the development of theoretical ideas about the details of the interaction of waves and particles in the magnetosphere leading to the generation of these previously unknown types of high-frequency VLF patches.

The second type of high-frequency short VLF bursty-patches was observed as long-lasting “dash-like” emissions observed at frequencies above ~7 kHz with typical spectrograms shown in Figs. 4 and 5. Actually, for the first time, these emissions have been observed at the Porojärvi station ($L=6.15$, Northern Finland) in January 1993 (Manninen 2005). The spectrograms show narrow-frequency emissions near 7 kHz with a constant or increasing frequency. They are shown in Fig. 13 which is adopted from Manninen (2005). At that time the digital sferics filter did not exist, but in mid-January, during morning hours there were not so many strong sferics received at high latitude. It allowed us to observe those emissions.

The spectral shape of the “dash-like” patches is much simpler compared to the spectra of the “triggered-like” emissions. We also found that they occur under more disturbed geomagnetic conditions than the “triggered-like” patches. Following the generally accepted conceptions, we suppose that both categories of high-frequency VLF bursty-patches are generated via electron cyclotron interaction between waves and energetic electrons near the magnetic equator of the radiation belts (e.g., Trakhtengerts and Rycroft 2008) at the frequencies controlled by the local f . It cannot be ruled out that other possibilities of wave generation can also develop in the magnetosphere (e.g., non-equatorial generation); however, this requires further theoretical and experimental studies.

Since the “triggered-like” patches are observed at lower frequencies than the “dash-like” ones, the latter ones should be generated at deeper L -shells than the first ones. Logically, to get to deeper L -shells, resonant electrons should have higher energies, explaining why the level of magnetic activity during the “dash-like” VLF patches is greater than during the “triggered-like” patches.

It is very important to remember that both types of VLF bursty-patches are observed at frequencies much higher than equatorial f_{ce} which is equal to ~5.4 kHz at $L\sim 5.5$. As such, VLF bursty-patches could not be emissions generated near the equatorial plane of the magnetosphere at the L -shell ($L\sim 5.5$) of KAN and propagating in a ducted manner to the station. The observed waves could be generated either at lower L -shells or in the non-equatorial region. We suppose that these emissions are generated at lower L -shells in the magnetosphere because that was confirmed by experimental results obtained by Titova et al. (2017), Demekhov et al. (2020), and Titova et al. (2022). Moreover, as far as we know there were no satellite VLF data recorded with waves at such high frequencies (>5–6 kHz) at the equatorial plane or in a non-equatorial region at $L > 5$. Studying VLF emissions simultaneously detected by Van Allen Probes (RBSP) spacecraft in the equatorial plane of the magnetosphere and at KAN, Titova et al. (2017) found a very good correlation between 8 and 10 kHz emissions, located at $L\sim 3.5$, where f_{ce} is equal to ~20.4 kHz. Based on RBSP-B satellite data analysis, they found that the high-frequency whistler waves at frequencies $> f_{ce}/2$ were observed simultaneously with an increase in low-energy electron fluxes with energies more than 102 eV, which had transverse anisotropy.

Moreover, simultaneously with this VLF patch, an enhancement of the plasma density or duct was detected by the RBSP-B spacecraft (Fig. 5 in Titova et al. 2017). Hence, below local $f_{ce}/2$ (below ~10 kHz) the whistler mode waves can be trapped in this duct which

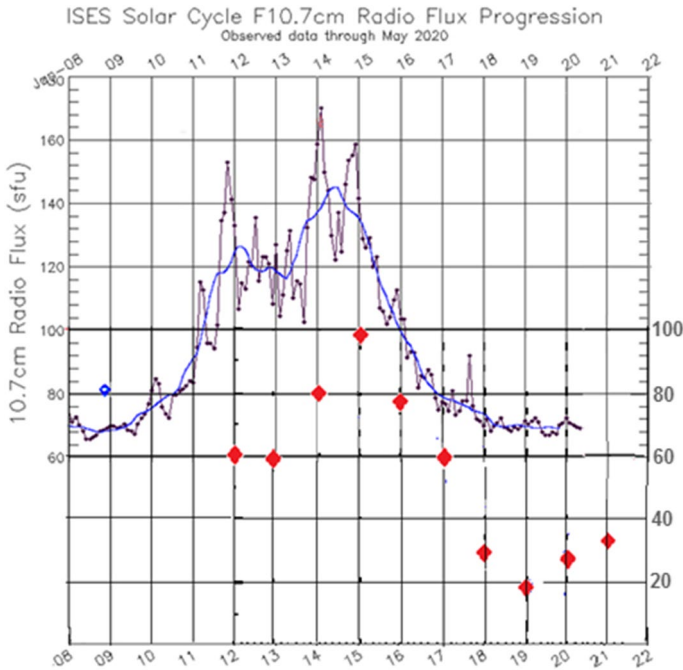


Fig. 14 Occurrence rate of VLF bursty-patches at frequencies above 6 kHz at KAN in 2012–2021 and the solar cycle activity (2008–2021) shown via F10.7 cm Radio Flux Progression

directs the waves to the ionosphere at L-shells much lower than the location of KAN. Ray tracing calculations (Titova et al. 2017) demonstrated that high-frequency waves at frequencies above $f_{ce}/2$ leave the duct at a distance of about one radius of the Earth. Apparently, from the end of a duct to the ground station, the higher frequency VLF waves propagate non-ducted as it was discussed in many papers (e.g., Nêmec et al. 2013; Martinez-Calderon et al., 2016; Titova et al. 2017; Demekhov et al. 2020). However, the details of that propagation are still unknown.

5 Final remarks

It is well known that the main source of all geomagnetic disturbances in the magnetosphere is solar wind disturbances originating from the Sun. Overall, VLF wave generation is related to these disturbances; however, we have established that both categories of VLF bursty-patches are observed under quiet and slightly disturbed geomagnetic conditions. Therefore, it is logical to assume that the average annual variations in the appearance of these waves will be in antiphase with solar activity. However, the variation of the number of days with any VLF bursty-patches, observed during the 10 winter seasons of 2011–2021 (December–January) and normalized to the total day numbers with the VLF occurrence, demonstrates a cycle

change looking similar to the variations of the solar cycle activity, as presented in Fig. 14. The same trend was found by Martinez-Calderon et al. (2021). The number of days with high-frequency VLF patches decreases with decreasing solar activity even though these emissions are typically generated under weak or moderate geomagnetic activity. This paradox, probably, can be explained by the presence of two competing processes: the VLF wave generation in the magnetosphere and their absorption during the cross-ionosphere propagation. A certain level of resonant magnetospheric electrons is required, the main source of which is the injection of charged particles from the tail of the magnetosphere caused by solar wind disturbances increased with an enhancement of geomagnetic activity: On the one hand, for the generation of VLF waves, a certain level of resonant magnetospheric electrons in the radiation belt is required, the main source of which is the injection from the tail of the magnetosphere increasing with geomagnetic activity. On the other hand, an increase in magnetic activity, associated with the solar wind disturbances, leads to an increase in the absorption of VLF waves during their cross-ionosphere propagation due to increasing energetic electron precipitation in the ionosphere measured on the ground by the riometer (Relative Ionospheric Opacity Meter [Little and Leinbach, 1959]) data as the enhanced riometer absorption up to a few dB. We may assume that for the ground-based occurrence of the VLF bursty-patch, the first process is more important.

6 Summary

1. Here, we presented a review of recent results of the analysis of high-frequency VLF bursty-patches at the ground-based station of Kannuslehto (KAN, $L \sim 5.5$) in Northern Finland. These emissions have rarely been observed earlier in the spectrograms on other ground stations as they are hidden by sferics from lightning discharges in the same frequency ranges. A special numeric filtering technics to reduce the sferics noise was applied to KAN data allowing to reveal these high-frequency VLF bursty-patches at frequencies much higher than the equatorial $0.5 f_{ce}$ corresponding to KAN.
2. VLF bursty-patches are mostly a daytime phenomenon observed during the local winter (darker season), similar to the occurrence of usual quasiperiodic emissions detected at lower frequencies ($f < 4\text{--}5$ kHz). High-frequency VLF bursty-patches exhibit a sequence of separate patches with a wide variety of spectral structures. The sequence of these patches can typically last several hours up to 6–7 h. This indicates that the conditions of their generation can exist in the magnetosphere for a relatively long time. The annual cyclical variations in bursty-patch occurrence are similar to the cyclical variations in solar activity.
3. We presented variable spectral structures of individual events of long-lasting series of VLF bursty-patches. Two different categories of bursty-patches have been established: (1) “*triggered-like*” VLF bursts at frequencies below 7–8 kHz with a very sharp onset and detected under very quiet geomagnetic conditions; (2) “*dash-like*” at frequencies above ~7–8 kHz detected under more disturbed geomagnetic conditions.

Acknowledgements The work of N.G. Kleimenova and L.I. Gromova was supported by the grant of Academy of Finland no. 308501. The filtered VLF KAN data are available at https://www.sgo.fi/pub_vlf/ as the power spectrograms in 24-h, 1-h, and 1-min intervals for all campaigns 2006–2021.

Funding Open Access funding provided by University of Oulu including Oulu University Hospital. This study was funded by the Academy of Finland (Research Council for Natural Sciences and Engineering, grant number 308501).

Declarations

Conflict of interest Author J. Manninen declares that he has no competing interests to declare that are relevant to the content of this article. Author N.G. Kleimenova has received research grants from the Academy of Finland. Author C. Martinez-Calderon declares that she has no competing interests to declare that are relevant to the content of this article. Author L.I. Gromova has received research grants from the Academy of Finland. Author T. Turunen declares that he has no competing interests to declare that are relevant to the content of this article.

Ethical approval This article does not contain any studies with human participants or animals performed by any of the authors.

Open Access This article is licensed under a Creative Commons Attribution 4.0 International License, which permits use, sharing, adaptation, distribution and reproduction in any medium or format, as long as you give appropriate credit to the original author(s) and the source, provide a link to the Creative Commons licence, and indicate if changes were made. The images or other third party material in this article are included in the article's Creative Commons licence, unless indicated otherwise in a credit line to the material. If material is not included in the article's Creative Commons licence and your intended use is not permitted by statutory regulation or exceeds the permitted use, you will need to obtain permission directly from the copyright holder. To view a copy of this licence, visit <http://creativecommons.org/licenses/by/4.0/>.

References

- Bergin A, Chapman SC, Gjerloev JW (2020) AE, DST, and their SuperMAG counterparts: The effect of improved spatial resolution in geomagnetic indices. *J Geophys Res Space Phys* 125:27828. <https://doi.org/10.1029/2020JA027828>
- Bespalov PA, Parrot M, Manninen J (2010) Short-period VLF emissions as solitary envelope waves in a magnetospheric plasma maser. *J Atmos Sol-Terr Phys* 72:1275–1281. <https://doi.org/10.1016/j.jastp.2010.09.001>
- Bespalov PA, Savina ON, Zharavina PD (2022) Special features of chorus excitation by means of the beam-pulse-amplifier mechanism in ducts of enhanced and depleted cold-plasma density with refraction reflection. *Cosmic Res* 60(1):15–22. <https://doi.org/10.1134/S0010952522010026>
- Carpenter DL (1968) Ducted whistler-mode propagation in the magnetosphere; a half-gyrofrequency upper intensity cut-off and some associated wave growth phenomena. *J Geophys Res* 73:2919–2928. <https://doi.org/10.1029/JA073i009p02919>
- Demekhov AG, Titova EE, Manninen J, Pasmanik DL, Lubchich AA, Santolik O, Larchenko AV, Nikitenko AS, Turunen T (2020) Localization of the source of quasiperiodic VLF emissions in the magnetosphere by using simultaneous 3 ground and space observations: a case study. *J Geophys Res Space Phys* 125:e27776. <https://doi.org/10.1029/2020JA027776>
- Demekhov AG, Titova EE, Manninen J, Nikitenko AS, Pilgaev SV (2021) Short periodic VLF emissions observed simultaneously by Van Allen Probes and on the ground. *Geophys Res Lett* 48:095476. <https://doi.org/10.1029/2021GL095476>
- Dingle B, Carpenter DL (1981) Electron precipitation induced by VLF noise bursts at the plasmopause and detected at conjugate ground stations. *J Geophys Res* 86(A6):4597–4606. <https://doi.org/10.1029/JA086iA06p04597>
- Engebretson MJ, Posch JL, Halford AJ, Shelburne GA, Smith AJ, Spasojevic M, Inan US, Arnoldy RL (2004) Latitudinal and seasonal variations of quasiperiodic and periodic VLF emissions in the outer magnetosphere. *J Geophys Res* 109:A05216. <https://doi.org/10.1029/2003JA010335>
- Fedorenko Y, Tereshchenko E, Pilgaev S, Grigoryev V, Blagoveshchenskaya N (2014) Polarization of ELF waves generated during “beating-wave” heating experiment near cutoff frequency of the Earth-ionosphere waveguide. *Radio Sci* 49:1254–1264. <https://doi.org/10.1002/2013RS005336>
- Helliwell RA (1965) Whistlers and related ionospheric phenomena. Stanford University Press
- Gjerloev JW (2012) The SuperMAG data processing technique. *J Geophys Res* 117(A9):A09213. <https://doi.org/10.1029/2012JA017683>

- Inan US, Bell TF (1977) The plasmapause as a vlf wave guide. *J Geophys Res* 82:2819–2827. <https://doi.org/10.1029/JA082i019p02819>
- Karpman VI, Kaufman RN (1982) Whistler wave propagation in density ducts. *J Plasma Phys* 27(2):225–238. <https://doi.org/10.1017/S0022377800026556>
- Kennel CF, Petschek HE (1966) Limit of stably trapped particle fluxes. *J Geophys Res* 71:1–28. <https://doi.org/10.1029/JZ071i001p00001>
- Little CG, Leinbach H (1959) The Riometer - A device for the continuous measurement of ionospheric absorption. *Proc of the IRE* 47(2):315–320. <https://doi.org/10.1109/JRPROC.1959.287299>
- Manninen J (2005) Some aspects of ELF_VLF emissions in geophysical research. Sodankyla Geophysical Observatory Publications. № 98. 177 p. Oulu Univ Press Finland. <https://www.sgo.fi/Publications/SGO/thesis/ManninenJyrki.pdf>
- Manninen J, Kleimenova NG, Kozyreva OV, Bespalov PA, Kozlovsky AE (2013) Non-typical ground-based quasiperiodic VLF emissions observed at L=5.3 under quiet geomagnetic conditions at night. *J Atmos Sol-Terr Phys* 99:123–128. <https://doi.org/10.1016/j.jastp.2012.05.007>
- Manninen J, Turunen T, Kleimenova N, Rycroft M, Gromova L, Sirvio I (2016) Unusually high frequency natural VLF radio emissions observed during daytime in Northern Finland. *Environ Res Lett* 11:124006. <https://doi.org/10.1088/1748-9326/11/12/124006>
- Manninen J, Turunen T, Kleimenova NG, Gromova LI, Kozlovsky AE (2017) A new type of daytime high-frequency VLF emissions at auroral latitudes (“Bird emissions”). *Geomagn Aeron* 57(1):32–39. <https://doi.org/10.1134/S0016793217010091>
- Manninen J, Kleimenova N, Turunen T, Nikitenko A, Gromova L, Fedorenko Yu (2021) New type of short VLF patches (“VLF birds”) above 4–5 kHz. *J Geophys Res Space Phys* 126(4):2. <https://doi.org/10.1029/2020JA028601>
- Martinez-Calderon C, Shiokawa K, Miyoshi Y, Keika K, Ozaki M, Schofield I, Kurth WS (2016) ELF/VLF wave propagation at subauroral latitudes: Conjugate observation between the ground and Van Allen Probes A. *J Geophys Res Space Phys* 121(A6):5384–5395. <https://doi.org/10.1002/2015JA022264>
- Martinez-Calderon C, Manninen JK, Manninen JT, Turunen T (2021) A review of unusual VLF bursty-patches observed in Northern Finland. *Earth, Planets and Space* 73:191. <https://doi.org/10.1186/s40623-021-01516-y>
- Nêmeç F, Santolík O, Parrot M, Pickett J, Cornilleau-Wehrlin HM (2013) Conjugate observations of quasi-periodic emissions by cluster and demeter spacecraft. *J Geophys Res Space Physics* 118(1):198–208. <https://doi.org/10.1029/2012JA018380>
- Ohya H, Shiokawa K, Miyoshi Y (2015) Daytime tweek atmospheric. *J Geophys Res Space Physics* 120(1):654–665. <https://doi.org/10.1002/2014JA020375>
- Rycroft MJ (1972) VLF emissions in the magnetosphere. *Radio Sci* 7:811–830. <https://doi.org/10.1029/RS007i008p00811>
- Rycroft MJ (1991) Interaction between whistler-mode waves and energetic electrons in the coupled system formed by magnetosphere, ionosphere and atmosphere. *J Atmos Terr Phys* 53:849–858. [https://doi.org/10.1016/0021-9169\(91\)90098-R](https://doi.org/10.1016/0021-9169(91)90098-R)
- Semenova VI, Trakhtengerts VY (1980) On specific features of the LF waveguide propagation. *Geomagn Aeron* 20(6):1021–1027
- Shiokawa K, Yokoyama Y, Ieda A, Miyoshi Y, Nomura R, Lee S, Connors M (2014) Ground-based ELF/VLF chorus observations at subauroral latitudes - VLF-CHAIN campaign. *J Geophys Res Space Physics* 119:7363–7379. <https://doi.org/10.1002/2014JA020161>
- Smith RL, Helliwell RA, Yabroff IW (1960) A theory of trapping of whistlers in field-aligned columns of enhanced ionization. *J Geophys Res* 65:1–20. <https://doi.org/10.1029/JZ065i003p00815>
- Strangeways HJ, Madden MA, Rycroft MJ (1983) High latitude observations of whistlers using three spaced goniometer receivers. *J Atmos Terr Phys* 45:387–399
- Titova EE, Demekhov AG, Manninen J, Pasmanik DL, Larchenko AV (2017) Localization of the sources of narrow-band noise VLF emissions in the range 4–10 kHz from simultaneous ground-based and Van Allen Probes satellite observations. *Geomagn Aeron* 57(6):706–718. <https://doi.org/10.1134/S0016793217060135>
- Titova EE, Shklyar DR, Manninen J (2022) Broadband whistler waves and differential electron fluxes in the equatorial region of the magnetosphere behind the plasmapause during substorm injections. *Geomagn Aeron* 62(4):399–412. <https://doi.org/10.1134/S0016793222040168>
- Trakhtengerts VYu (1963) On the mechanism of VLF radiation generation on the external radiation belt of the Earth. *Geomagn Aeron* 3(3):442–451
- Trakhtengerts VYu, Rycroft MJ (2008) Whistler and Alfvén mode cyclotron masers in space. Cambridge University Press

Yearby KH, Smith AJ (1994) The polarization of whistlers received on the ground near $L = 4$. *J Atmos Terr Phys* 56:1499–1512

Publisher's Note Springer Nature remains neutral with regard to jurisdictional claims in published maps and institutional affiliations.